Acta Microscopica Vol. 28, No.2, 2019, pp.364-372

Application of Electron Microscope in the Unconstrained Compressive Strength and Fractal Dimension of the Calcareous Sand with Curing Agent

Shuai Yang
School of Ocean Science and Engineering, Shanghai Maritime University, Shanghai 201306, China

Wenbai Liu*
School of Ocean Science and Engineering, Shanghai Maritime University, Shanghai 201306, China
**Corresponding author (E-mail: liuwb8848@163.com)*

Abstract
The calcareous sand from an island of the South China Sea is solidified by curing agent, and the unconfined compressive strength is measured by the unconfined compressive strength test. The microscopic images of calcareous sand are gained by Scanning Electron Microscope (SEM). The image is dealt with by Image-Pro Plus (IPP), and the fractal dimension is computed which includes particle size fractal dimension D_{ps}, particle surface fractal dimension D_{pr} and aperture fractal dimension D_{bs}. The connection between unconfined compressive strength and fractal dimension is to be done. The research indicates that the curing agent can improve the compressive strength of the calcareous sand, that is to say, adding the curing agent can effectively improve the properties of soil. The unconfined compressive strength has a linear relation with the fractal dimensions. Compared with the other two fractal dimensions, the function of the particle surface fractal dimension D_{pr} on the compressive strength is greater.

Key words: Calcareous Sand, Curing Agent, Unconfined Compressive Strength, Scanning Electron Microscope, Fractal Dimension

1. Introduction

Calcareous sand, as a special geotechnical medium formed by marine organisms, is widely distributed in the South China Sea. Calcareous sand, as a natural foundation, is mostly found in civil and national defense projects in the South China Sea. Its characteristics are that the bearing capacity of foundation is low and the building load is small. However, with China's strategic goal of "Building a Marine Power", China will increase the development and construction of the South China Sea islands, in which the construction and use of wharfs, airport runways and various civilian military buildings will encounter problems of calcareous sand foundation. Liu Chongquan [2] studied the physical and mechanical properties of calcareous sand，Liu Hanlong [3] studied the liquefaction characteristics of calcareous sand，Zhu Changqi [4] analyzed the internal pore characteristics of calcareous sand structure. These studies show that calcareous sand is a special geotechnical material with internal pore, irregular shape and easy particle breakage, so its mechanical properties are different from ordinary sand. Qin Yue[6] and Jiang Hao[7] carried out the experimental study of calcareous sand model piles. A large number of experiments and engineering cases show that the traditional pile foundation engineering experience could not be applied to calcareous sand. Therefore, measures should be taken to improve the mechanical properties of soil foundation in the South China Sea.

Many scholars have done a lot of research in the field of improving soil properties. Liu Hanlong [1] did research on dynamic behaviors of MICP-treated calcareous sand in cyclic tests. The studies of Ivanov [14] and Van Paassen [15] have proved that MICP can improve the strength and stiffness of soil in laboratory and large-scale tests. Through scanning electron microscopy and simple chemical tests, DeJong[16] found that MICP cement was calcite, and the calcite precipitation was distributed between particles, which enhanced the shear strength of sand. All of the above studies have limitations. They all use microbial induction to improve the mechanical properties of soil. The measure has harsh sampling conditions, complex operation, high material cost and lack of good economic benefits. Moreover, the above studies do not establish a good correlation between macro and micro, lack of quantitative macro and micro studies, mostly qualitative analysis between macro and micro, lack of reliable reference data basis.

In this paper, the properties of the calcareous sand are effectively improved by adding curing agent in calcareous sand, so as to replace the traditional method of pile foundation engineering in the field of ocean engineering. The microscopic images of calcareous sand are gained by SEM, then the image is dealt with by Image-Pro Plus. Under certain conditions, the compressive strength and fractal dimension of the solidified calcareous sand are obtained, and the quantitative relationship between macro and micro is established to build a

bridge for macro and micro research.

2. Test Materials and Test Methods

2.1. Test Materials

The test soil samples were cleaned with calcareous sand from an island reef in the South China Sea. After drying, a small amount of large particle impurities in the undisturbed sand were removed to form the soil samples for the test. The average particle size d_{50} = 0.32 mm, the inhomogeneity coefficient C_u = 2.18, the curvature coefficient C_c = 0.92, the maximum void ratio e_{max} = 1.75, and the minimum void ratio e_{min} = 1.27.

The curing agent in the test is a self-made curing agent. The curing agent contains a variety of materials, including ordinary portland cement, lime (CaO), sodium sulfonate, acrylamide and so on. The components of cement are shown in Table 1.

Table 1. The components of cement (%)

SiO_2	Al_2O_3	Fe_2O_3	CaO	MgO	K_2O	Na_2O	P_2O_3	TiO_2	SO_3
21.04	6.94	2.36	61.27	1.32	1.02	0.27	0.12	0.38	2.31

2.2. Test Method

The whole experimental process is to add curing agent (6%, 8%, 10%, 12%) into calcareous sand to make samples, and put the samples into the curing box for maintenance. Then the unconfined compressive test is developed to obtain the compressive strength of the sample. Meanwhile, the micro image is gained by the SEM microstructure test of the sample. Then the micro-images are dealt with by IPP software, and the micro-structure parameters are obtained. Finally, the quantitative analysis between compressive strength and microstructure parameters is discussed.

In the sample preparation process, 6%, 8%, 10% and 12% curing agent are added to the South China Sea's calcareous sand, then 20% water is added to mix well. Then mix the soil sample into 70.7 mm x 70.7 mm x 70.7 mm x 70.7 mm mould in two or three times, each time needs to be tampered with tamping rod. Then the whole soil sample and mould are put into the curing box with temperature of 20 degrees Celsius and humidity of 99%. The curing period is 7 days, 14 days, 21 days, 28 days, 42 days and 90 days. Finally, the sample is taken out of the mould.

The SEM test is done by field emission scanning electron microscope (ER-SEM) made in Japan. The sample is dehydrated and dried by oven drying method, and then the small sample of 10 * 10 *20mm is slowly cut out with a knife for observation.

The micro image of the South China Sea's solidified calcareous sand is dealt with by using IPP. Hang Li [5], Xu Riqing[6,9],Zhen Zhiheng[10] have introduced specific practices.

3. Test Result

3.1. Unconfined Compression Test Result

The unconfined compressive strength of the calcareous sand under different curing periods and curing agent content is shown in Tab.2. It illustrates along with the curing age growth, the unconfined compressive strength also increases.

Table 2. The unconfined compressive strength of the calcareous sand (Mpa)

Curing age T/d	Curing agent content λ/%			
	6	8	10	12
7	1.596	2.574	3.906	4.771
14	1.885	2.752	4.120	5.178
21	2.228	3.122	4.685	5.727
28	2.427	3.707	4.975	5.967
42	2.512	3.889	5.112	6.022
90	2.514	3.890	5.101	6.147

It is due to the hydration reaction of the curing agent. The hydration reaction equation is as follows:

$$3CaO \cdot SiO_2 + 7H_2O \rightarrow 3CaO \cdot 2SiO_2 \cdot 3H_2O + 3Ca(OH)_2$$

$$2CaO \cdot SiO_2 + 5H_2O \rightarrow 3CaO \cdot 2SiO_2 \cdot 3H_2O + 3Ca(OH)_2$$

The hydrated calcium silicate produced by hydration reaction has strong cementation. The formed calcium hydroxide is also filled in the pores, which plays a certain role in the solidification of calcareous sand. Moreover, the other part of calcium hydroxide comes from the hydration reaction of lime. The hydration reaction equation is as follows:

$$CaO + H_2O \rightarrow Ca(OH)_2$$

In addition, the calcium hydroxide reacts with CO_2 and water to form calcite crystals, which have strong cementation.

In conclusion, the curing agent can improve the properties of the calcareous sand, which is due to the cementation of hydrated products such as calcium silicate, calcium hydroxide and calcite crystals generated by hydration reaction.

3.2. Image Calculation Results

The SEM image of the calcareous sand is dealt with by image processing software, and the data related to particle and pore are extracted from the graph for analysis. Then the fractal dimensions are computed by using Matlab according to relevant formulas. Fractal Dimensions are quantitatively analyzed.

Measuring the particle contour line of solidified dredger fill with length measuring ruler of ε, the number of required measuring ruler is N(ε). By changing ε, the different N(ε) can be obtained. A series of ε and N(ε) as points are depicted on the double logarithmic coordinate diagram, and the negative value of the slope of the straight line fitting through these points is the particle surface fractal dimension.

$$D_{pr} = -\lim_{\varepsilon \to 0} \frac{\ln N(\varepsilon)}{\ln \varepsilon} \quad (1)$$

Where: D_{pr}—particle surface fractal dimension

ε — length of measuring ruler measuring the particle contour line of solidified dredger fill

N(ε)—number of measuring ruler

The particle surface fractal dimension of solidified calcareous sand under different curing periods and curing agent content is shown in Tab.3. It illustrates that along with the increase of curing age, the particle surface fractal dimension decreases.

Table 3. The surface fractal dimension of solidified calcareous sand

curing age T/d	curing agent content λ/%			
	6	8	10	12
7	1.242	1.245	1.244	1.246
14	1.231	1.235	1.234	1.230
21	1.219	1.220	1.219	1.217
28	1.212	1.211	1.211	1.209
42	1.204	1.201	1.199	1.197
90	1.205	1.199	1.199	1.196

The number of aperture which is larger than r is N (≥r), r values will be changed, and a series of N (≥r) will be obtained. N (≥r) and r are depicted on the double logarithmic coordinate diagram. The negative value of the slope of the straight line fitting through these points is the aperture fractal dimension.

$$D_{bs} = \frac{-\ln N(\geq r)}{r} \quad (2)$$

Where: D_{bs} —aperture fractal dimension

r —aperture

N—aperture number

The aperture fractal dimension of the solidified calcareous sand under different periods and curing agent content is shown in Tab.4. It illustrates that along with the curing age growth, the aperture fractal dimension increases.

Table 4. The aperture fractal dimension of solidified calcareous sand

Curing age T/d	Curing agent content λ/%			
	6	8	10	12
7	1.477	1.481	1.494	1.493
14	1.536	1.541	1.552	1.554
21	1.596	1.609	1.612	1.619
28	1.623	1.626	1.632	1.635
42	1.633	1.634	1.641	1.643
90	1.635	1.633	1.641	1.644

Particle size fractal dimension D_{ps} is similar to the calculation principle and method of aperture fractal dimension.

The Particle size fractal dimension of the solidified calcareous sand under different periods and curing agent content is shown in Tab.5. It illustrates that as the curing age rises, the mean equivalent pore diameter decreases.

Table 5. The particle size fractal dimension of solidified calcareous sand

Curing period T/d	Curing agent content λ/%			
	6	8	10	12
7	1.432	1.451	1.481	1.485
14	1.401	1.431	1.462	1.460
21	1.390	1.404	1.421	1.419
28	1.379	1.388	1.390	1.389
42	1.374	1.369	1.366	1.363
90	1.372	1.370	1.365	1.362

4. Relation between Unconfined Compressive Strength and Fractal Dimensions

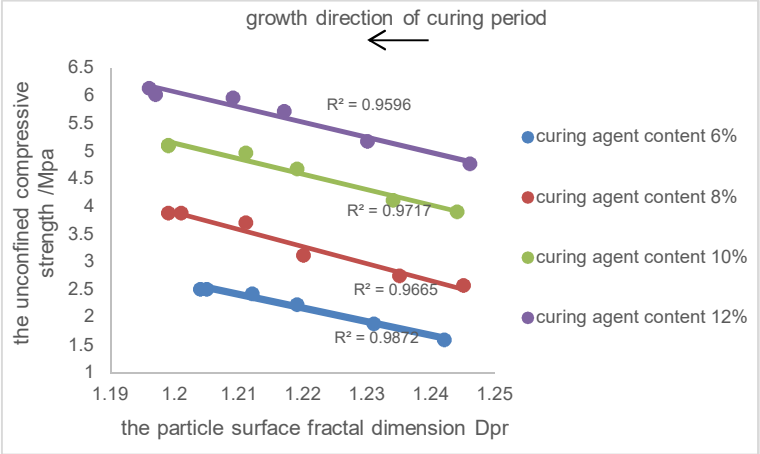

Figure 1. The relation between the unconfined compressive strength and particle surface fractal dimension.

Table 6. Linear relation between unconfined compressive strength and particle surface fractal dimension

Particle surface fractal dimension Dpr			
Curing agent content λ/%	The relation between unconfined compressive strength and particle surface fractal dimension	R^2	Slope K
6	y = -24.801x + 32.422	0.9872	24.801
8	y = -31.063x + 41.173	0.9665	31.063
10	y = -27.834x + 38.543	0.9717	27.834
12	y = -27.345x + 38.882	0.9596	27.345

The connection between the unconfined compressive strength and particle surface fractal dimension is shown in Fig.1. Fig.1 shows that under the same fly ash content, along with the decrease of the particle surface fractal dimension, the unconfined compressive strength increases linearly. Thereinto, the particle surface fractal dimension decreases with the increase of curing age, because the hydration products bind the soil particles together, and the fluctuation between the soil particles is reduced. It indicates that the hydration products between soil particles increase the contact area, thus the compressive strength rises.

The linear relation between the unconfined compressive strength and particle surface fractal dimension is

showed in Table 6. Table 6 shows the linear formula between compressive strength and particle surface fractal dimension when curing agent content is 6%, 8%, 10% and 12%.

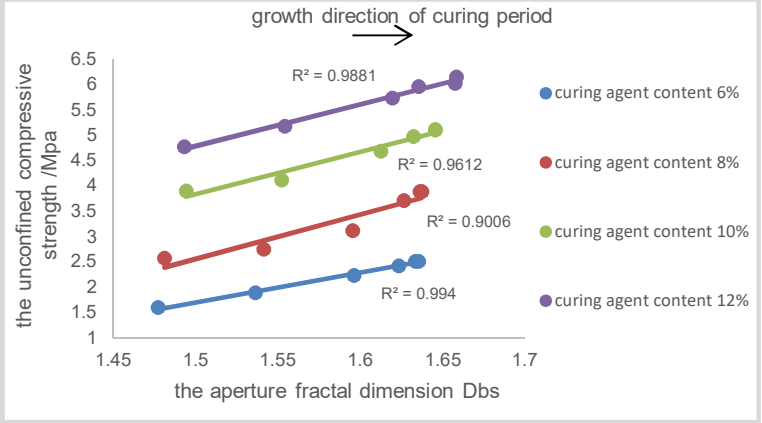

Figure 2. The relation between the unconfined compressive strength and aperture fractal dimension

Table 7. Linear relation between unconfined compressive strength and aperture fractal dimension

Aperture fractal dimension Dbs			
Curing agent content λ/%	The linear relation between unconfined compressive strength and aperture fractal dimension	R^2	Slope K
6	y = 5.8878x - 7.1287	0.994	5.8878
8	y = 8.8296x - 10.681	0.9006	8.8296
10	y = 8.3571x - 8.6937	0.9612	8.3571
12	y = 8.2218x - 7.5414	0.9881	8.2218

The connection between the unconfined compressive strength and aperture fractal dimension is shown in Fig.2. Fig.2 illustrates that under the same fly ash content, as the aperture fractal dimension rises, the unconfined compressive strength increases linearly. The aperture fractal dimension rises with the increase of curing age, because the curing agent and some hydration products fill the soil sample pore, which reduce the pore size. It shows that the curing agent and the hydration products generated by hydration reaction are filled in the pores between the calcareous sand particles, which changes the pore structure, thus increasing the compressive strength.

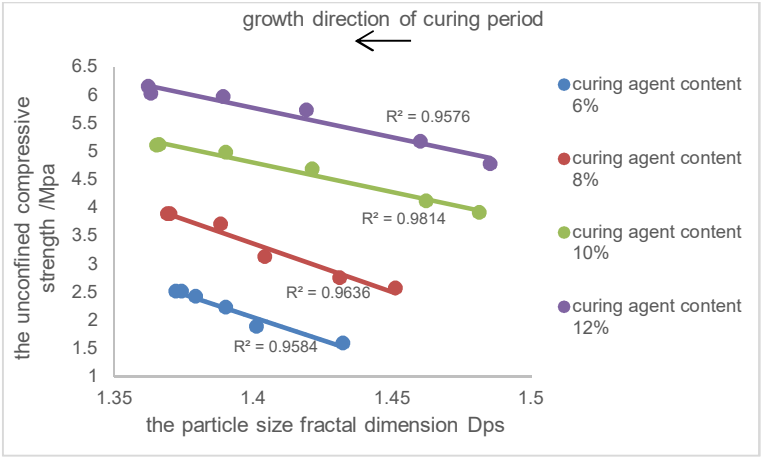

Figure 3. The relation between the unconfined compressive strength and particle size fractal dimension

The linear relation between the unconfined compressive strength and aperture fractal dimension is showed in Table 7. Table 7 also shows the linear formula between compressive strength and aperture fractal dimension when curing agent content is 6%, 8%, 10% and 12%. Similarly, it indicates that the aperture fractal dimension can be determined through a certain amount of curing agent and a certain curing age, and then the compressive strength of solidified calcareous sand can be calculated by using the above linear relationship.

Table 8. Linear relation between unconfined compressive strength and particle size fractal dimension

Particle size fractal dimension Dps			
Curing agent content λ/%	The linear relation between unconfined compressive strength and particle size fractal dimension	R^2	Slope K
6	y = -16.279x + 24.843	0.9584	16.279
8	y = -17.257x + 27.519	0.9636	17.257
10	y = -10.486x + 19.479	0.9814	10.486
12	y = -10.42x + 20.359	0.9576	10.42

The connection between the unconfined compressive strength and particle size fractal dimension is shown in Fig.3. Fig.3 indicates that under the same fly ash content, as the particle size fractal dimension decreases, the unconfined compressive strength increases linearly. Thereinto，the particle size fractal dimension reduces with the increase of curing age. It is because the hydration products are wrapped on the surface of the soil particles, the situation changes soil gradation. This illustrates that the hydration products are attached to the surface of calcareous sand particles, the condition improves soil gradation, and thus the compressive strength rises.

The linear relation between the unconfined compressive strength of the calcareous sand and particle size fractal dimension is showed in Table 8. Table 8 also shows the linear formula between compressive strength and particle size fractal dimension when curing agent content is 6%, 8%, 10% and 12%. In the same way, the compressive strength of the solidified calcareous sand can be calculated by using the above formula.

In conclusion, the hydration products produced by hydration reaction are attached to the surface of sand particles or filled between soil particles in the solidified calcareous sand. The condition improves soil gradation and changes pore structure, and the compressive strength of the solidified calcareous sand rises.

Moreover, through a certain amount of curing agent and a certain curing time, the fractal dimensions can be determined, and the compressive strength of the calcareous sand can be calculated by using the macro-micro relationship obtained from the experiment. In this way, we can explain the causes of macro-changes with micro-values more scientifically and intuitively, so as to build a bridge for macro-micro research.

Table 9. Linear relation between unconfined compressive strength and fractal dimensions

Fractal dimensions			
Particle surface fractal dimension Dpr			
Curing content λ/%	The linear relation between unconfined compressive strength and fractal dimensions	R^2	Slope K
6	y = -24.801x + 32.422	0.9872	24.801
8	y = -31.063x + 41.173	0.9665	31.063
10	y = -27.834x + 38.543	0.9717	27.834

12	y = -27.345x + 38.882	0.9596	27.345
Aperture fractal dimension Dbs			
6	y = 5.8878x - 7.1287	0.994	5.8878
8	y = 8.8296x - 10.681	0.9006	8.8296
10	y = 8.3571x - 8.6937	0.9612	8.3571
12	y = 8.2218x - 7.5414	0.9881	8.2218
Particle size fractal dimension Dps			
6	y = -16.279x + 24.843	0.9584	16.279
8	y = -17.257x + 27.519	0.9636	17.257
10	y = -10.486x + 19.479	0.9814	10.486
12	y = -10.42x + 20.359	0.9576	10.42

The linear relation between unconfined compressive strength of the calcareous sand and fractal dimensions is shown in Table 9. It illustrates that compared with the particle surface fractal dimension Dpr, the slope of the linear relation between the compressive strength and the aperture fractal dimension Dbs and the particle size fractal dimension Dps is relatively small, which indicates that compared with the other two fractal dimensions, the function of the particle surface fractal dimension Dpr on the compressive strength is greater.

5. Discussion

In this paper, we show that the curing agent can improve the properties of the calcareous sand, and the unconfined compressive strength has a linear relation with the fractal dimensions. Through this experiment, we find that through a certain amount of curing agent (6%, 8%, 10%, 12%) and a certain curing time (7d, 14d, 21d, 28d, 42d, 90d), the fractal dimensions can be determined. And the unconfined compressive strength of the calcareous sand can be calculated by using the macro-micro relationship obtained from the experiment. It also indicates that the mechanical properties of the calcareous sand can be effectively improved by adding curing agent.

Compared with the research of Liu Hanlong [1], the research of the scholar lacks quantitative analysis between macro and micro, some are only qualitative analysis, while our research is quantitative analysis between macro and micro. Moreover, the scholar's method to improve the calcareous sand is microbial induction method, which is complex to operate, harsh sample preparation conditions and high cost of materials. However, our research on the use of curing agents is simple, cost-effective and it can also improve the properties of the calcareous sand.

The past studies have shown that the experience of traditional pile foundation engineering could not be applied to the calcareous sand. And the past research methods are only qualitative analysis between micro and macro research. Now with this research, we can get the numerical relationship between macro and micro, not only the trend of change between them, so that we can explain the reason of the compressive strength's change with the numerical change of micro-structure parameters more scientifically and intuitively.

Although there are important discoveries revealed by the paper, there are also limitations. First, the research is based on unconfined compressive strength test, the test conditions are unconfined, but the actual project is limited, so the research provides a theoretical basis. Second, the amount of curing agent used in this paper is only 6%, 8%, 10%, 12%, which needs further promotion.

Finally, one subject that remains to be explored is how to better apply the measures of adding curing agent to the ocean engineering construction, and whether the factors of the calcareous sand particle breakage will affect the research results.

6. Conclusions

The unconfined compressive strength of the calcareous sand is measured by the unconfined compressive strength test. The microscopic images are gained by SEM. The image is dealt with by IPP. The connection

between unconfined compressive strength and fractal dimension is to be done. The research shows that:

1) Curing agent can improve the compressive strength of the calcareous sand, that is to say, adding curing agent can effectively improve the properties of calcareous sand. It enhances the compressive strength of the calcareous sand due to the cementation of hydrated products such as hydrated calcium silicate, calcium hydroxide and calcite crystals produced by hydration reaction.

2) The curing agent improves the compressive strength of the soil, because the hydration products produced by the hydration reaction of the curing agent adhere to the surface of calcareous sand particles or fill between the soil particles. And the structure formed enhances the connection strength between the soil particles, which makes the loose soil samples cemented into a whole structure.

3) The unconfined compressive strength of the calcareous sand has a linear relation with the fractal dimensions. By establishing the quantitative relationship between macro and micro, the fractal dimensions can be determined through a certain amount of curing agent (6%, 8%, 10%, 12%) and a certain curing time (7d, 14d, 21d, 28d, 42d, 90d). By using the macro-micro relationship obtained from experiments, the unconfined compressive strength of the calcareous sand can be calculated and the bridge can be built for macro-micro research.

Acknowledgments

Financial support for this study was provided by the National Natural Science Foundation of China (51078228) and the National Marine public welfare industry research special funds of China (201105024-5).

References

[1] Liu Han-Long, Xiao Peng, Xiao Yang, Wang Jian-Ping, Chen Yu-Min, Chu Jian (2018) “Dynamic Behaviors of MICP-treated Calcareous Sand in Cyclic Tests”, *Chinese Journal of Geotechnical Engineering*, 40(1), pp.38-45.

[2] Liu Chong-Quan, Yang Zhi-Qiang, Wang Ren (1995) “The Present Condition and Development in Studies of Mechanical Properties of Calcareous Soils”, *Rock and Soil Mechanics*, 16(4), pp.74–84.

[3] Liu Han-Long, Hu Ding, Xiao Yang, Chen Yumin (2015) “Test Study on Dynamic Liquefaction Characteristics of Calcareous Sand”, *Journal of Disaster Prevention and Mitigation Engineering*, 35(6), pp.707–711.

[4] Zhu Chang-Qi, Chen Hai-Yang, Meng Qing-Shan, Wang Ren (2014) “Microscopic Characterization of Intra-Pore Structures of Calcareous Sands”, *Rock and Soil Mechanics*, 33(7), pp.1831–1836.

[5] Xu Riqing, Deng Weiwen, Xubo, Lai Jianping, Zhan Xuegui. (2015) “Quantitative Analysis of Soft Clay Three-dimensional Porsity Based On SEM Image Information”, *Journal of Earth Science and Environment*, 3, pp.104-110.

[6] Qin Yue, Meng Qin-Shan, Wang Ren, Zhu Chang-Qi (2015) “A Study on Bearing Characteristics of Single Pile in Calcareous Sand Based on Model Experiment”, *Rock and Soil Mechanics*, 36(6), pp.1714–1720.

[7] Jiang Hao, Wang Ren, Lü Ying-Hui, Meng Qing-Shan (2010) “Test Study of Model Pile in Calcareous Sands”, *Rock and Soil Mechanics*, 31(3), pp.780–784.

[8] Xu Riqing, Xu Liyang, Deng Weiwen, Zhu Yihong (2015) “Experimental Study on Soft Clay Contact Area Based on SEM and IPP”, *Journal of Zhejiang University (Engineering Science)*, 08, pp.1417-1425.

[9] Zhen Zhiheng, Gao Jianwei (2015) “The Microscopic Characteristic Analysis of Red Bed Mudstone Modified Soil Based on IPP”, *Transportation Science and Technology*, 08, pp.124-127.

[10] Tang Yixin, Liu Hanlong, Zhu Wei (2000) “Study on Engineering Properties of Cement-Stabilized Soil”, *Chinese Jounal of Geotechnical Engineering*, 22(5), pp.549-554.

[11] Shi Bin, Jiang Hongtao (2001) “Research on the Analysis Techniques for Clayey Soil Microstructure”, *Chinese Journal of Rock Mechanics and Engineering*, 20(6), pp.864-870.

[12] Fang Qingjun, Hong Baoning (2014) “Research Progress at Geotechnical Micro and Mesostructure”, *Science Technology and Engineering*, 14(17), pp.143-149.

[13] Wang Dongxing, Xu Weiya (2012) “Research on Strength and Durability of Sediments Solidified with High Volume Fly Ash”, *Rock and Soil Mechanics*, 33(12), pp.3659-3663.

[14] Ivanov V, Chu J, Stabnikov V, Li B. (2015) “Strengthening of soft marine clay using bioencapsulation”, *Marine Georesources & Geotechnology*, 33(4), pp.325–329.

[15] Van Paassen L A, Ghose R, Van Der L T J M, Van Der S W R L, Van Loosdrecht M C M. (2010) “Quantifying Biomediated Ground Improvement by Ureolysis: Large-Scale Biogrout Experiment”, *Journal of Geotechnical and Geoenvironmental Engineering*, 136(12), pp.1721–1728.

[16] Dejong J T, Fritzges M B, Nüsslein K. (2006) “Microbially Induced Cementation to Control sand Response to Undrained Shear”, *Journal of Geotechnical and Geoenvironmental Engineering*, 132(11), pp.1381–1392.

[17] Druvic Lemus-Espinoza (2018) "Mortalidad por micosis sistémicas no asociadas a VIH, en Venezuela. Período 1995-2013", *Investigación Clínica,* 59(2), pp.107-117.
[18] Qirui Fu, Shaomin Huang, Huan Yu, Jinkun Zeng, Qingxi Chen, Jiangxing Zhuang, Qionghua Chen (2019) "Apoptosis Induced by ESC-3Through Notch Signaling Pathway and Mitochondrial Membrane Potential (ΔΨm) in Liver Cancer", *Acta Microscopica,* 28(1),pp.62-71.
[19] Katherin Rosal, Aliana Useche (2018) "La epigalocatequina-3-galato induce apoptosis en plaquetas", *Investigación Clínica,* 59(2), pp.146-154.
[20] Kang, L.; Du, H.L.; Du, X.; Wang, H.T.; Ma, W.L.; Wang, M.L.; Zhang, F.B. (2018) "Study on dye wastewater treatment of tunable conductivity solid-waste-based composite cementitious material catalyst", *Desalination and Water Treatment,* 125, pp. 296-301.
[21] Yingyi Zhang, Wenjie Ni (2018) "Yungang Li. Effect of Siliconizing Temperature on Microstructure and Phase Constitution of Mo–MoSi2 Functionally Graded Materials", *Ceramics International*, 44(10), pp 11166-11171.
[22] Kai Wang, ShengZhe Zhou, YanTing Zhou, Jun Ren, LiWei Li and Yong Lan (2018) "Synthesis of Porous Carbon by Activation Method and its Electrochemical Performance", *International Journal of Electrochemical Science,* 13(11), pp. 10766-10773.